2

Sonographic Imaging of the Peripheral Nerves in Patients with Type 2 Diabetes Mellitus

Tsuneo Watanabe, Shin-ichi Kawachi[1] and Toshio Matsuoka
Department of Sports Medicine and Sports Science,
Gifu University Graduate School of Medicine
[1]Departments of Diabetes and Endocrinology,
Gifu University Graduate School of Medicine
Japan

1. Introduction

The World Health Organization estimates that more than 220 million people worldwide have diabetes mellitus (DM). This figure is estimated to more than double by 2030 (Wild et al., 2004). In Japan, the number of diabetic patients has increased to 8 million, and it is assumed that 35% to 45% of diabetic patients have diabetic symmetric polyneuropathy (DPN). Advanced DPN causes serious complications, such as diabetic foot ulcers, gangrene, and Charcot joint, all of which worsen the quality of life of diabetic patients (Ogawa et al., 2006). Therefore, early detection of nerve dysfunction is important to provide appropriate care for patients with DPN (Chudzik et al., 2007). The diagnosis of diabetic neuropathy is based primarily on characteristic symptoms and is confirmed with nerve conduction studies (NCS), which are time-consuming, slightly invasive, and occasionally not well tolerated for repeated evaluations (Colak et al., 2007). In contrast, ultrasonographic examinations can be performed to assess peripheral nerves with less discomfort and have already been used for the evaluation of several disorders of the peripheral nervous system such as carpal tunnel syndrome (Wiesler et al., 2006a; Abe et al., 2004; Jayaraman et al., 2004; Duncan et al., 1999; Lee et al., 1999), cubital tunnel syndrome (Okamoto et al., 2000; Wiesler et al., 2006b), and traumatic nerve lesions (Cartwright., 2007; Peer et al., 2001). High-resolution diagnostic ultrasonography (US) has improved greatly, allowing for evaluation of minute peripheral nerves (Fornage., 1993; Solbiati et al., 1985). We previously showed that the cross-sectional area (CSA) of the median nerve in the carpal tunnel of patients with DPN is greater than that of controls and correlates with NCS (Watanabe et al., 2009). Furthermore, it appears that the percentage of the hypoechoic area of the peripheral nerves was significantly greater in patients with lower motor nerve conduction velocity (MCV) and DM than in controls or patients with higher MCV and DM (Watanabe et al., 2010).

The purpose of this chapter is to review the current knowledge regarding the overview and diagnosis of the most common forms of neuropathy in type 2 DM. Furthermore, our current sonographic technique and preliminary studies are presented for some cases. In this chapter,

we focus mainly on a simple and noninvasive approach to the evaluation of peripheral nerves in patients with type 2 DM. Although the exact mechanisms contributing to our study have not been clearly identified and are not the main focus of this chapter, they will be discussed in brief.

2. Clinical aspects of diabetic neuropathy

Diabetic neuropathy is a neuropathic disorder that is associated with DM. This condition is thought to result from both diabetic microvascular injury involving small blood vessels that supply nerves and macrovascular conditions that can culminate in DM. More than 80% of patients with clinical diabetic neuropathy have a distal, symmetrical form of the disorder (Said., 2007). In general, the symptoms included numbness, burning feet, pins-and-needles sensations, and lightning pains. These symptoms start in the feet go on to affect more proximal parts of the lower limbs, and eventually affect the distal parts of the upper limbs.

The unified clinical criteria and classification for DPN do not represent the international standard because the causes of peripheral nerve disorders associated with DM are complex and probably involve a variety of causative mechanisms. In this chapter, DPN is classified into 3 groups (hyperglycemic neuropathy, symmetric polyneuropathy, and focal and multifocal neuropathy) according to the classification of the Thomas et al (1997). This classfication is the easiest. The most common of these groups seen in the clinical setting is symmetric distal polyneuropathy.

3. Pathology of diabetic neuropathy

Abnormalities reported in diabetic neuropathy include axonal degeneration in nerve fibers, primary demyelination resulting from Schwann cell dysfunction, secondary segmental demyelination related to impairment of axonal control of myelination, remyelination, proliferation of Schwann cells, atrophy of denervated bands of Schwann cells, onion-bulb formations, and hypertrophy of the basal lamina. Early morphological changes include minimal alteration of myelinated and unmyelinated fibers and axonal regeneration (Yagihashi et al., 2007; Said et al., 2007).

The pathophysiology of DPN is multifactorial and involves genetic, environmental, behavioral, metabolic, neurotrophic, and vascular factors (Vink et al., 1999; Oates, 2002; Vincent, et al., 2002; Perkins, et al., 2003). The vascular concept of peripheral diabetic neuropathy implies that diabetes-induced endothelial dysfunction with a resultant decrease in nerve blood flow, vascular reactivity, and endoneurial hypoxia plays a key role in functional and morphological changes in the diabetic nerve (Cameron et al., 2001). Endothelial changes in the vasa nervorum have been attributed to multiple mechanisms, including increased aldose reductase activity, nonenzymatic glycation and glycoxidation, activation of protein kinase C, oxidative–nitrosative stress, and changes in arachidonic acid and prostaglandin metabolism (Cameron et al., 2001). The complex and interrelated effects of hyperglycemia include increased metabolic flux through the polyol pathway with consequent sorbitol and fructose accumulation and reduced sodium-potassium ATPase levels, altered fatty acid metabolism, alterations in the redox state, reduced myoinositol and sodium-potassium ATPase activity, accumulation of advanced glycated end products, accelerated neuronal apoptosis, immunological alterations, changes in blood flow, and

increased oxidative stresses. The exact mechanisms of DPN are uncertain, but may involve activation of the polyol pathway due to hyperglycemia; the polyol pathway is considered to play a major role in diabetic neuropathy (Greene, et al., 1987). Excellent reviews of this information are available in previous publications.

4. NCS

Diagnosis of DPN on clinical grounds alone is not accurate, and it is difficult to detect small alterations in neuropathies (Feldman et al, 1994; Perkins et al, 2001). Therefore, as a surrogate measure, NCS are widely used as an evaluation of DPN. NCS measure the ability of peripheral nerves to conduct electrical signals, and this ability is impaired when pathological changes are present in the myelin, nodes of Ranvier, and axons. Routine NCS include evaluation of the motor function of the median, ulnar, peroneal, and tibial nerves, and evaluation of the sensory function of the median, ulnar, radial, and sural nerves. Velocities are universally reported in meters per second, motor amplitudes in millivolts, and sensory amplitudes in microvolts. These measurements of upper- and lower-limb motor and sensory nerve functions show the presence, distribution, and severity of peripheral nerve disease (Albers, et al., 1995).

The attribution of peripheral nerve dysfunction to either primary demyelination or primary axonal loss is usually based on nerve conduction velocity and action potential amplitude data. In general, demyelination is indicated by a decreased nerve conduction velocity, conduction block, or increased temporal dispersion, whereas axonal loss is indicated by a reduction in the amplitude or area of the sensory nerve action potential (SNAP) or compound muscle action potential (CMAP). However, there has been considerable disagreement in terms of the clinical and the electrophysiological criteria for the diagnosis of DPN.

Recently, various calculated indices such as the residual latency, terminal latency index, and modified F-wave ratio were introduced as more sensitive electrophysiological tools than a conventional NCS in patients with diverse types of peripheral neuropathies (Attarian et al, 2001; Kaplan, et al, 1978; Radziwill et al, 2003).

5. Sonography

5.1 Sonographic features of normal peripheral nerves

US is a widely utilized diagnostic tool for gynecological purposes and examinations of the heart and intra-abdominal and superficial organs. With the advancement of sonographic resolution, normal peripheral nerves also can be clearly demonstrated. US is a useful technique for the investigation of a number of musculoskeletal disorders. Although US has the well-known advantages of low cost, accessibility, portability, noninvasiveness, and multiplanar imaging, one of its most important diagnostic advantages over other techniques is considered to be its real-time imaging capability, allowing for dynamic evaluation of the musculoskeletal field (Khoury et al., 2007).

US can be used to determine the location, extent, type of lesion as well as the presence of nerve swelling and inflammation. Major peripheral nerves in the extremities, such as the median, ulnar, radial, sciatic, and posterior tibial nerves can be seen using conventional US performed with 5- to 12-MHz probes (Stokvis et al., 2009). In controls, peripheral nerves are seen as hypoechoic neuronal fascicles surrounded by echogenic connective tissue (Silvestri

et al., 1995). The basic units of the peripheral nerve consist of a neural fiber embedded in the endoneurium. Because the endoneurium is too thin to reflect the sound beam, it is hypoechogenic on the US scan. The neural fascicle consists of several neural fibers and is embedded in a capsule called the perineurium. This capsule consists of connective tissue, vessels, and lymphatic ducts and is thick enough to reflect the sound beam, resulting in hyperechoic lines on the US scan. The trunk of the peripheral nerve consists of several neural fascicles and is embedded in a thicker membrane called the epineurium, which is seen as bold echogenic lines on the US. Therefore, a peripheral nerve is seen as several parallel hyperechoic lines and bold hypoechoic lines on longitudinal images and as a faveolate pattern on transverse images (Fig 1).

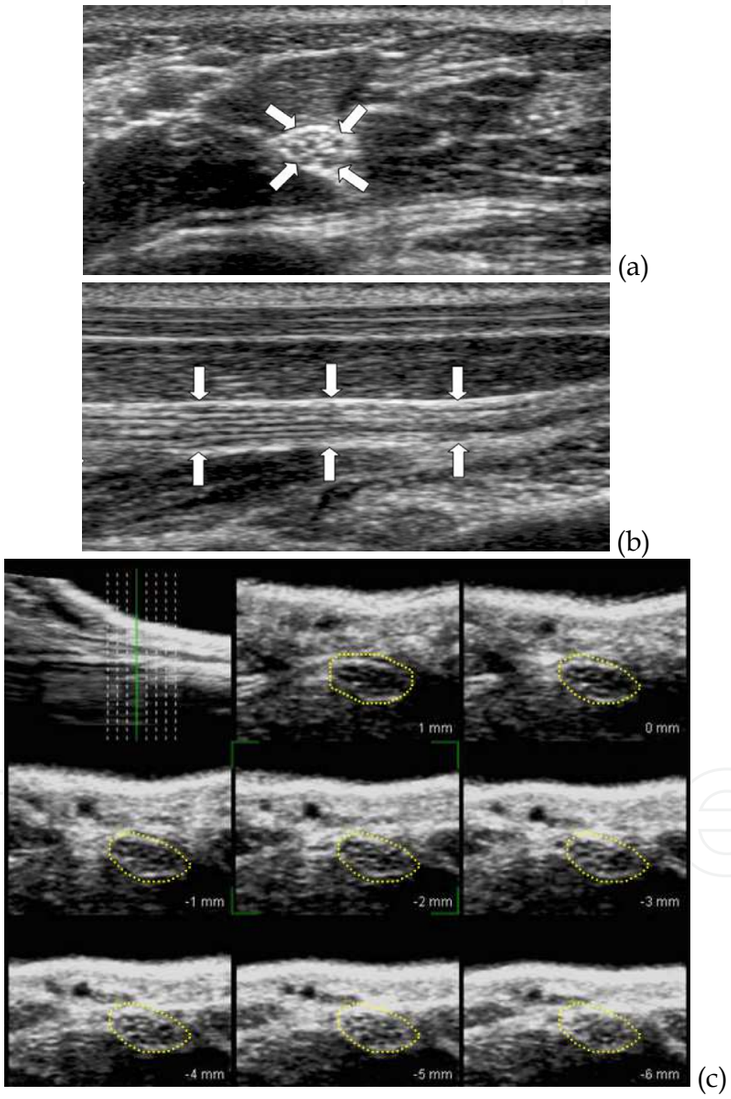

(a) (b) (c)

Fig. 1. Sonographic imaging of the median nerve. Transverse sonogram of the median nerve in 5cm proximal to the wrist (a), and longitudinal sonogram of the median nerve (b). Multi-slice views using three-dimensional volumetric ultrasonography images (c). The transverse planes at continuous segment of the median nerves are visualized.

5.2 Sonographic features of the peripheral nerves in patients with type 2 DM

We previuosly reported that peripheral nerves in patients with low MCV and type 2 DM showed enlarged and hypoechoic patterns as compared with those of controls or patients with high MCV and type 2 DM. There are 2 sonographic methods of measuring nerve CSA: the indirect method (ellipsoid formula) and direct method (tracing). Recently, Alemán et al.(2008) reported that median nerve CSA measurements are reproducible by either the direct or indirect method when a standardized ultrasonographic examination protocol is applied. Sernik et al. (2008) also reported a high correlation (r = 0.99) between the areas calculated by the indirect and direct methods.

In patients with DPN, peripheral nerves showed enlarged and hypoechoic patterns. Figure 2 shows sonographic images of several nerves in the controls and in patients with type 2 DM. The CSAs of the median, ulnar, and tibial nerves in patients with DM were significantly larger than those in controls. It is likely that these findings reflect the pathological changes, although the pathogenesis of nerve enlargement and increased percentage of the hypoechoic area in peripheral nerves is uncertain because our study did not include histological evidence. In a 1H-nuclear magnetic resonance study, Suzuki et al. (1994) reported that sorbitol and the sodium accumulation caused by an increase in sorbitol may be major contributors to the increase in intracellular hydration. It has further been hypothesized that peripheral nerves are swollen in individuals with DM because of increased water content related to an increase in the aldose reductase-mediated conversion of glucose to sorbitol. We hypothesize that the increase in the hypoechoic area of peripheral nerves in diabetic patients may be because of increased water content, which is also a cause of enlargement of peripheral nerves.

5.3 Assessment of the internal echo of the peripheral nerves

The ultrasonographic images of the peripheral nerves were saved as JPEG files and transferred to a personal computer for analysis. The monochrome US image was quantized to 8 bits (i.e., 256 gray levels). The brightness of the pixels ranged from 0 (black) to 255 (white). Histogram analysis in US has been expected to offer an objective index for estimating the echo intensity, such as in the diagnosis of fatty liver or hepatitis (Lee et al., 2006; Osawa et al., 1996). The region of interest was set to cover the entire nerve, excluding its hyperechoic rim. We used the percentage of the hypoechoic area as the index after the effects of gain shift on echo intensity in the median nerve were confirmed (Fig. 3).

The normal appearance of a peripheral nerve should be readily recognized. Peripheral nerves consist of multiple hypoechoic bands corresponding to neuronal fascicles, which are separated by hyperechoic lines that correspond to the epineurium. Thus, the value obtained by the discriminant analysis method of Otsu was used as a threshold level for the analysis of the percentage of the hypoechoic area because the echogenicity of peripheral nerves was obtained as a graded echo density from black to white. Otsu's method (1979), which selects a global threshold value by maximizing the separability of the classes in gray levels, is one of the better tequniques for image segmentation. Mathematically, this can be expressed as:

$$p_i = \frac{f_i}{N},\ p_i \geqq 0,\ \sum_{i=1}^{L} p_i = 1. \tag{1}$$

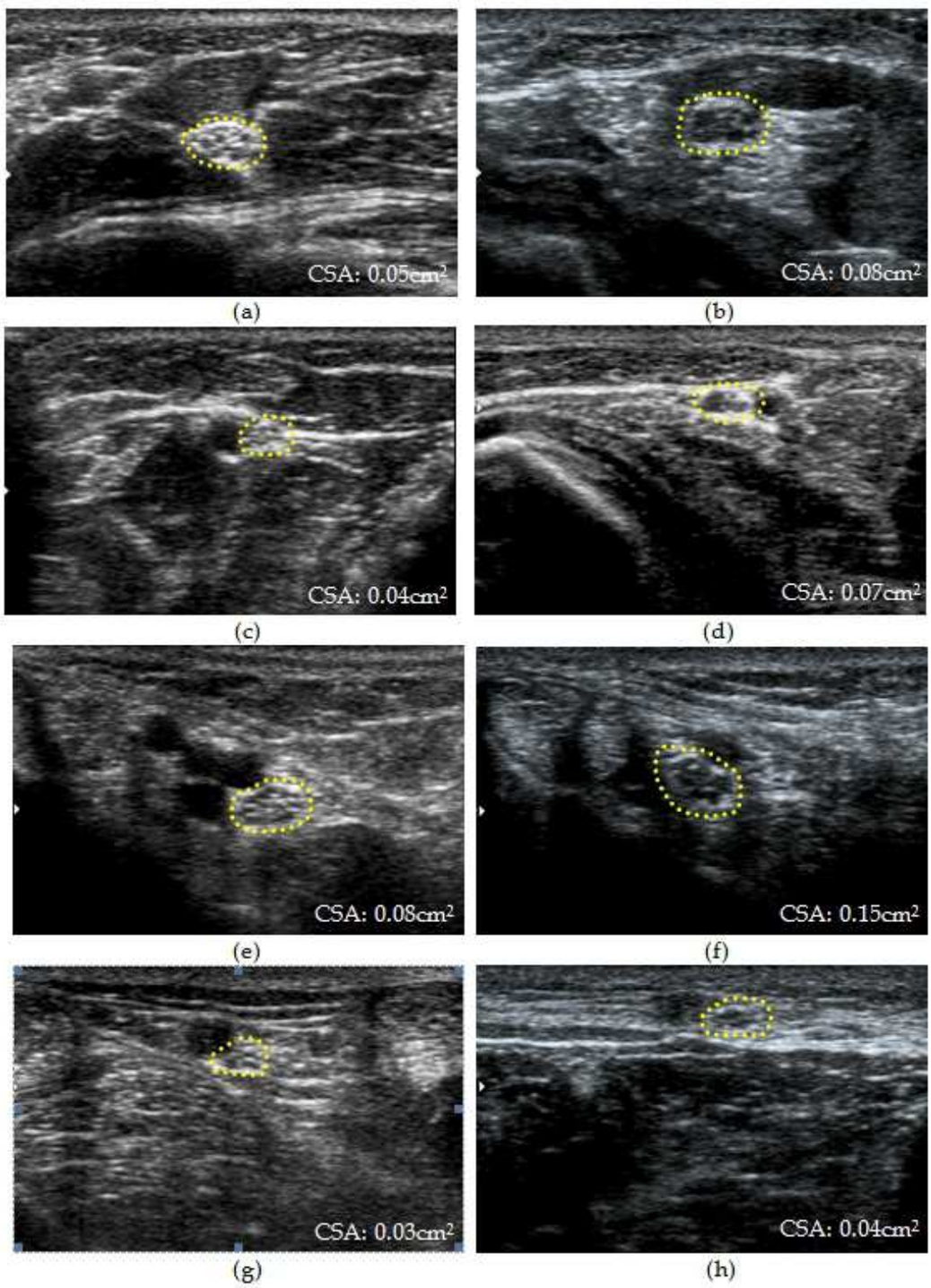

Fig. 2. Comparison of the nerves in controls and in diabetic patients. Transverse image of the median nerve in control' wrist (a), and in diabetic patient's wrist (b). Transverse image of the ulnar nerve in control' wrist (c), and in diabetic patient's wrist (d). Transverse image of the tibial nerve in control' ankle (e), and in diabetic patient's ankle (f). Transverse sonogram of the sural nerve in control' ankle (g), and in diabetic patient's ankle (h).

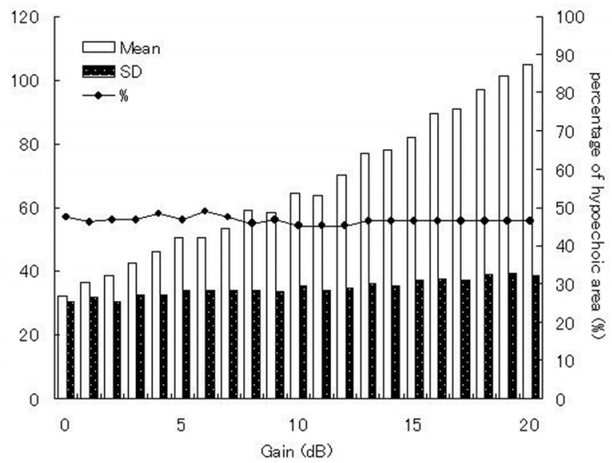

Fig. 3. The effects of the gain shift on the echo intensity in the median nerve. Open bars showed a change of mean, closed bars showed a change of SD, and solid line connecting solid circles showed a change of percentage according to the gain shift.

Assume that the image can be represented in L gray levels (1, 2,…, L). If the number of pixels at level i is denoted by f_i, then the total number of pixels equals $N = f_1 + f_2 + \ldots + f_L$. If an image can be divided into 2 classes (C_1 and C_2) by a threshold at level t, where class C_1 consists of gray levels from 0 to t, and class C_2 contains the other gray levels with $t + 1$ to L, then the cumulative probabilities (w_1 and w_2) and mean levels (μ_1 and μ_2) for classes C_1 and C_2, respectively, are given by

$$w_1 = \sum_{i=1}^{t} p_i , \tag{2}$$

$$w_2 = \sum_{i=t+1}^{L} p_i , \tag{3}$$

and

$$\mu_1 = \sum_{i=1}^{t} i p_i / w_1 , \tag{4}$$

$$\mu_2 = \sum_{i=t+1}^{L} i p_i / w_2 . \tag{5}$$

Otsu selects an optimal threshold t^* that maximizes the between-class variance σ_B^2 in Eq. (6) based on the discriminant analysis, where μ_T is the mean intensity of the image.

$$t^* = \arg_{1 \le t \le L} \max\{\sigma_B^2(t) \mid \sigma_B^2 = w_1(\mu_1 - \mu_T)^2 + w_2(\mu_2 - \mu_T)^2\} \tag{6}$$

and

$$\mu_T = \sum_{i=1}^{L} ip_i \,. \tag{7}$$

The percentage of the hypoechoic area was studied using computer analysis. Using ImageJ software, the amount of the hypoechoic area falling below the threshold echo intensity was calculated. In our computerized method, the flowchart of the echo intensity evaluation process is demonstrated in Figure 4.

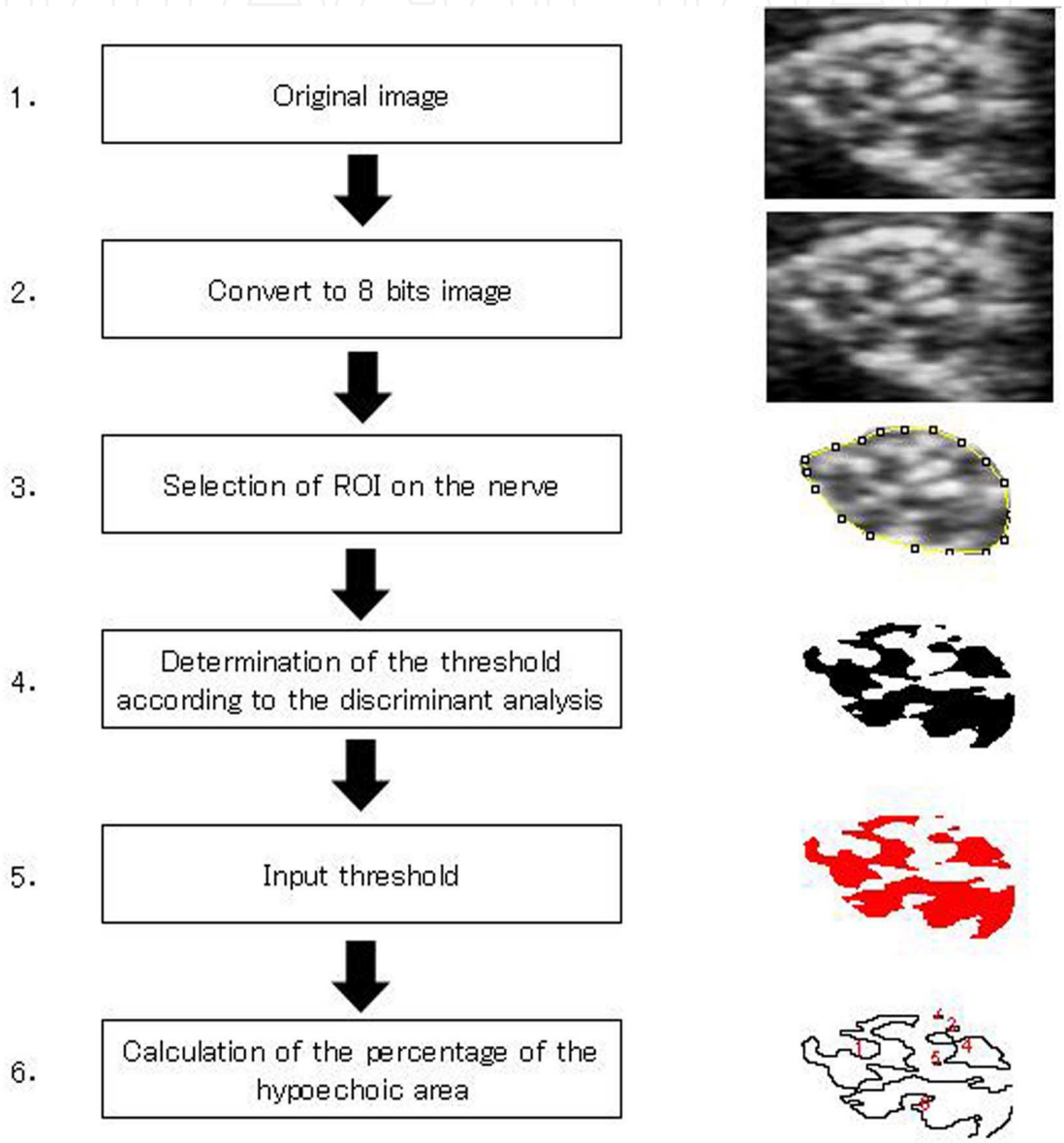

Fig. 4. Illustration of the working flow of the evaluation of the echo intensity.

Representative sonographic images and three-dimensional graphic using ImageJ software of diabetic patients and controls are shown in Fig 5.

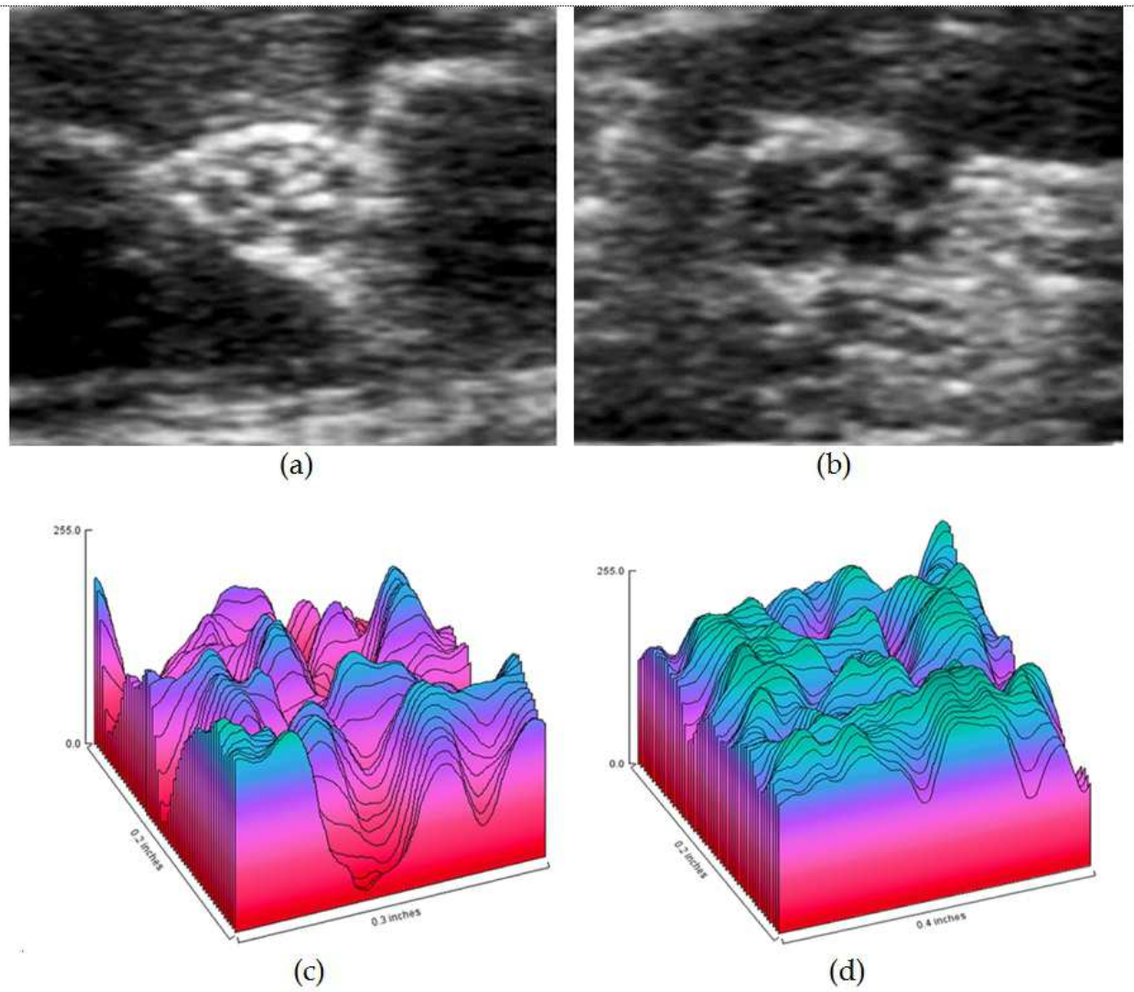

Fig. 5. Distributions of the echo intensity in the median nerve. Transverse sonogram of the median nerve in a control participant's wrist (a). Transverse sonogram of the median nerve in a diabetic patient's wrist (b).Three-dimensional graphic of the distribution of the echo intensity in the control's wrist (c). Three-dimensional graphic of the distribution of the echo intensity in the diabetic patient's wrist (d). Hypoechoic area was displayed "light blue", and hyperechoic area was displayed "pink".

6. Sonography and NCS in patients with type 2 DM

6.1 Relationship between sonography and NCS

We studied 144 peripheral nerves (40 median, 40 ulnar, 40 tibial, and 24 sural nerves) of 40 subjects who underwent both US and NCS (unpublished data). Overall, 20 type 2 diabetes patients [10 men and 10 women; age range, 50-88 years (mean, 68.5 ± 10.7 years)] and 20 healthy volunteers [12 men and 8 women; age range, 26-59 years (mean, 40.0 ± 12.3 years)] were enrolled in this study. All participants whose wrists had symptoms of carpal tunnel syndrome were excluded from the study. This study was approved by the Institutional Review Board of Gifu University Hospital, and informed consent was obtained from all participants.

Ultrasonographic examination was performed by a board-certified sonographer who was blinded to the knowledge of the electrodiagnostic results. A 6.0- to 14.0-MHz linear array probe was used (portable real-time apparatus: Aplio XG; Toshiba Medical Systems, Japan). All subjects were seated on the examination table with their arms on a pillow and fingers semi-extended during examination of the median or ulnar nerves, and in the prone position during examination of the tibial and sural nerves. The CSA of the median nerve was measured at the carpal tunnel (MA) and at 5 cm proximal to the wrist (MB). The CSA of the ulnar nerve was measured at 5 cm proximal to the wrist (UA). The CSA of the tibial nerve was measured at the posterior medial malleolus (TA). The CSA of the sural nerve was measured at the lower third of the crus (SA). US images were quantitatively analyzed using the ImageJ software (National Institutes of Health, USA). We evaluated the relationship between the US and NCS results.

Routine NCS were performed using conventional procedures and standard electromyography (Neuropack MEB-2200; Nihon Kohden Corp., Japan). All examinations were performed in a room with an ambient temperature of 25°C. The skin surface temperature in all cases was 31°C to 34°C. Mann-Whitney *U* test was used to compare data between the 2 groups. Pearson's correlation coefficients were used to investigate the correlation of CSA and the percentage of the hypoechoic area with several NCS parameters. Results are given as mean ± SD, and statistical significance was assessed at $P < 0.05$.

The US and NCS results of diabetic patients and controls are shown in Table 1. The CSAs in the patients with DM group were 0.13 ± 0.05 cm^2 in the MA, 0.09 ± 0.03 cm^2 in the MB, 0.0.7 ± 0.02 cm^2 in the UA, 0.18 ± 0.04 cm^2 in the TA, and 0.05 ± 0.01 cm^2 in the SA. The CSAs in the controls were 0.08 ± 0.02 cm^2 in the MA, 0.07 ± 0.02 cm^2 in the MB, 0.04 ± 0.01 cm^2 in the UA, 0.10 ± 0.03 cm^2 in the TA, and 0.04 ± 0.01 cm^2 in the SA. The CSAs was a significant increase in the diabetic patients compared with that in the controls, with the exception of the sural nerve. The percentage of the hypoechoic area was significantly increased in the diabetic patients compared with that in the controls ($P < 0.05$). The MCV and sensory nerve conduction velocity of all nerves in the diabetic patients showed a significant decrease compared with those in the controls ($P < 0.001$). The CMAP and SNAP of all nerves in the diabetic patients showed a significant decrease compared with those in the controls, with exception of the CMAPs of both the median and tibial nerves ($P < 0.001$). On the other hand, distal latency (DL) was significantly lesser in the diabetic patients than in the controls, with the exception of the sensory ulnar and motor tibial nerves.

The relationships between US findings and NCS parameters are shown in Figure 6. The motor DL period of the median nerve was divided into 3 groups: DL of <3.5 ms; DL of 3.5 to 4.0 ms; and DL of >4.0 ms. The MCV of the median nerve was also divided into 3 groups: MCV of <50 m/s; MCV = 50 to 55 m/s; and MCV of >55 m/s. The categorization of subjects into tertiles of DL yielded 3 separate groups. Compared with the first tertile, the CSAs of the median nerve increased significantly with each tertile. Moreover, after combining tertiles of DL and MCV, even more comprehensive CSA stratification was possible, with all-cause CSA ranging from 0.07 cm^2 in subjects in the lowest tertile of both parameters to 0.17 cm^2 in subjects in the highest tertile (Fig. 6a). The hypoechoic area of the median nerve also increased significantly with each tertile. The hypoechoic area of the median nerve stratification was 52.5% in subjects in the highest tertile of both parameters (Fig. 6b). These results correlated with the electrophysiological severity.

Parameters	Nerve	Controls	Patients with type 2 DM
Sonographic measurements (CSA)			
MA (cm^2)	*Median*	0.08 ± 0.02	0.13 ± 0.05***
MB (cm^2)	*Median*	0.07 ± 0.02	0.09 ± 0.03**
UA (cm^2)	*Ulnar*	0.04 ± 0.01	0.07 ± 0.02***
TA (cm^2)	*Tibial*	0.10 ± 0.03	0.18 ± 0.04***
SA (cm^2)	*Sural*	0.04 ± 0.01	0.05 ± 0.01
Sonographic measurements (echo intensity)			
MB (%)	*Median*	43.7 ± 5.1	50.0 ± 9.3*
UA (%)	*Ulnar*	43.6 ± 4.1	49.6 ± 10.6*
TA (%)	*Tibial*	44.8 ± 4.5	51.4 ± 7.5*
SA (%)	*Sural*	40.4 ±7.1	48.8 ± 3.7*
Electrophysiologic measurements			
MCV (m/s)	*Median*	59.9 ± 4.4	50.7 ± 5.7***
DL (ms)	*Median*	3.3 ± 0.5	4.5 ± 1.3***
CMAP (mV)	*Median*	11.2 ± 3.7	11.6 ± 4.4
SCV (m/s)	*Median*	69.1 ± 8.6	57.3 ± 5.7***
DL (ms)	*Median*	2.7 ± 0.4	3.3 ± 0.4***
SNAP (uV)	*Median*	38.3 ±11.7	12.5 ± 8.3***
MCV (m/s)	*Ulnar*	64.7± 6.1	52.1± 6.7***
DL (ms)	*Ulnar*	2.5 ± 0.4	2.9 ± 0.5*
CMAP (mV)	*Ulnar*	14.9 ± 3.8	9.4 ± 2.5***
SCV (m/s)	*Ulnar*	72.0 ± 5.4	61.7 ± 10.5***
DL (ms)	*Ulnar*	3.3 ± 0.7	3.9 ± 0.8
SNAP (uV)	*Ulnar*	20.4 ± 10.0	6.3 ± 2.9***
MCV (m/s)	*Tibial*	49.4 ± 2.4	40.3 ± 5.1***
DL (ms)	*Tibial*	3.9 ± 0.5	4.4 ± 0.9
CMAP (mV)	*Tibial*	16.1 ± 5.3	13.1 ± 6.9
SCV (m/s)	*Sural*	55.7± 2.5	49.1± 5.3***
DL (ms)	*Sural*	2.5 ± 0.1	2.9 ± 0.3***
SNAP (uV)	*Sural*	10.3± 4.1	3.6 ± 2.5***

Table 1. US and NCS measurements of controls and patients with type 2 DM (unpublished data).

Mann-Whitney U test: *P<0.05 versus controls; **P<0.01 versus controls; ***P<0.001 versus controls.

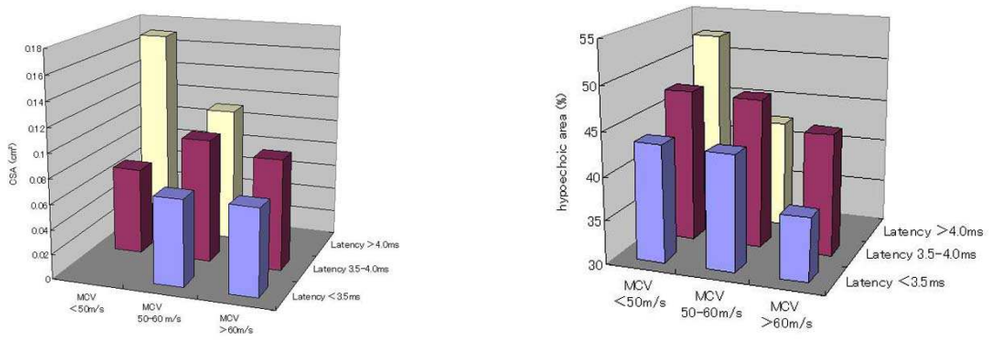

(a) (b)

Fig. 6. Relationships of between US and NCS parameters in the median nerve. Stratification of CSA by combining tertiles of DL and MCV (a). Stratification of hypoechoic area by combining tertiles of DL and MCV (b).

6.2 Comparison of diagnostic ability between US and NCS parameters

NCS are widely used for the diagnosis of DPN. The examinations are deemed to be objective, reliable, and sensitive, and can be used as statistical instruments or surrogate endpoints for neuropathy in large clinical investigations of DPN (Diabetes Control and Complications Trial Research Group., 1995; Cornblath et al., 1999; Dyck et al., 1991). NCS have also been recommended in the medical literature as the "gold standard" with which to evaluate and validate other screening tests that are used to diagnose peripheral neuropathy. We aimed to determine the best diagnostic criterion for diagnosing DPN by US and NCS. A receiver operating characteristic (ROC) curve was generated for each parameter in the US and NCS examinations, and areas under the curve (AUC) were determined. The ROC curves are plots of the true-positive rate (sensitivity) against the false-positive rate (1.0 – specificity) for the different possible cutoff points of a diagnostic test. To determine the accuracy of detection of DPN, we calculated and compared the sensitivity and specificity of both US and NCS.

In our preliminary study, the CSA at TA in the tibial nerve had the best diagnostic accuracy for DPN of all the sonographic examinations. The ROC curves of the CSA at TA revealed that the AUC was 0.919 ($P < 0.001$) with an optimal cutoff value of 0.145 cm^2, yielding 80% sensitivity and 94% specificity. For the NCS, the SNAPs had the best diagnostic accuracy for DPN; each nerve had an extremely high AUC (median nerve, 0.971; ulnar nerve, 0.944; and sural nerve, 0.938; $P < 0.001$). These cutoffs also yielded very good sensitivity (93% - 94%) and specificity (80% to 92%). Some investigators have reported that sural nerve dysfunction is the most common indicator of peripheral nerve dysfunction, is the first to be affected, and correlates most closely with the neuropathological findings (Dyck et al., 1985; Dyck., 1988; Redmond et al., 1992). Dyck et al. (1985) found that the peroneal motor nerve had the highest degree of abnormality, followed by the sural, median sensory, and median motor nerves. Karsidag et al. (2005) also reported that the most affected nerves were the sural sensory, peroneal motor, posterior tibial motor, median motor, ulnar motor, median sensory, and ulnar sensory nerves. In our study, the sural nerve had a high AUG, as reported in previous reports. Furthermore, the CSA at TA showed the most effective parameter in the US examinations; it was suggested that the most useful and practical

nerves for electrophysiological and sonographical studies in diabetic patients are the lower extremity nerves.

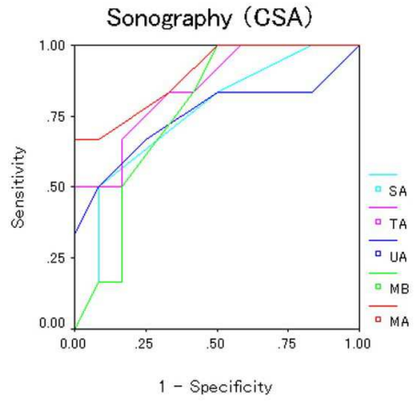

(a)

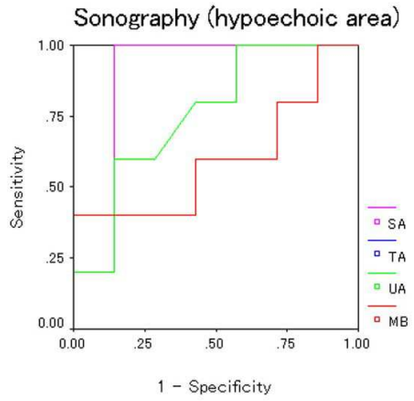

(b)

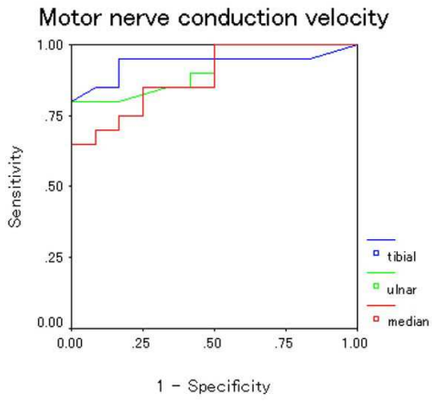

(c)

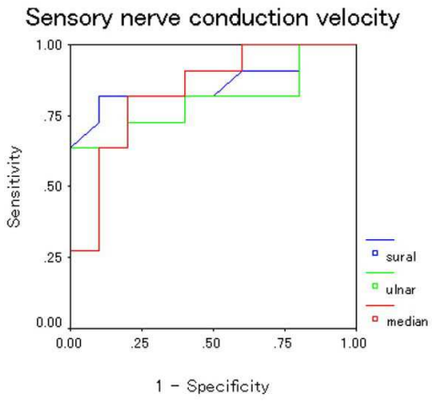

(d)

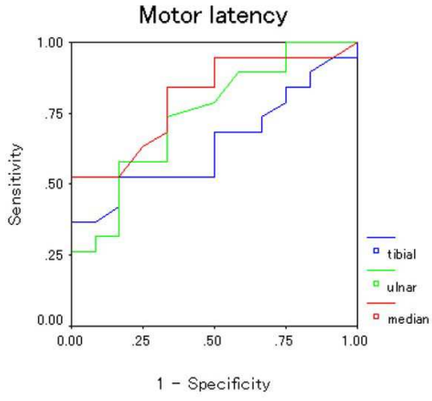

(e)

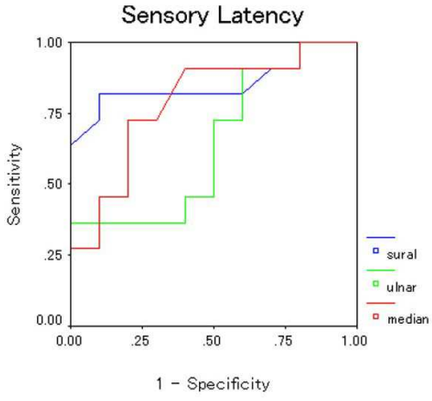

(f)

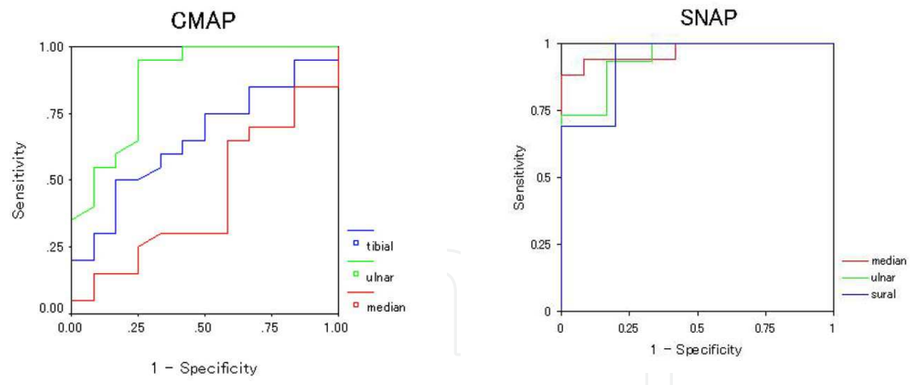

(g) (h)

Fig. 7. Receiver operating characteristic curves fitted for difference modality. (a) When the ROC curve was fitted using CSA results of US, CSA at the TA was most effective. (b) When the ROC curve was fitted using hypoechoic area of US, SA at the sural nerve was most effective. (c) When the ROC curve was fitted using MCV results of NCS, MCV of the tibial nerve was most effective. (d) When the ROC curve was fitted using SCV results of NCS, SCV of the sural nerve was most effective. (e) When the ROC curve was fitted using motor DL results of NCS, latency of the median nerve was most effective. (f) When the ROC curve was fitted using sensory DL results of NCS, latency of the sural nerve was most effective. (g) When the ROC curve was fitted using CMAP results of NCS, CMAP of the ulnar nerve was most effective. (h) When the ROC curve was fitted using SNAP results of NCS, SNAP of the median nerve was most effective.

According to the ROC curve analysis, to investigate whether the use of US and NCS could accurately determine the presence of DPN, we compared the sensitivity and specificity of different parameters. Both sensitivity and specificity were higher in NCS than in US. These results were consistent with the current status that NCS is widely accepted as the more sensitive system of evaluation of polyneuropathy. Although sonographic measurements have insufficient sensitivity and specificity compared with those of the NCS, the ROC curves showed that AUCs were as high as 0.681 to 0.919, yielding 43% to 94% sensitivity and 50% to 94 % specificity. We promote the possibility of using sonography to diagnose DPN.

7. Conclusion

In this chapter, we have reviewed the current knowledge of neuropathy in type 2 DM and have introduced a sonographical examination for DPN. Based on our present data, it appears that both size and hypoechoic area of nerves were increased in patients with type 2 DM compared with controls. US is a noninvasive method that can be used to evaluate detailed nerve structures. The results from this preliminary study indicate that US might be considered as a valuable tool for the evaluation of DPN. In this work, we focused on the development of an objective method of quantitative analysis of echogenicity changes in peripheral nerves over a clarification of the mechanism. Some limitations of our study should be mentioned. First, a relatively small number of participants were studied and no adjustments were made for age differences. Second, our study was an ultrasonographic examination only; therefore, exactly what causes an increased hypoechoic area or CSA

remains unknown. Furthermore, we must describe the property of sound waves. The property depends on both the object and the matrix in which it occurs, in that it relates to changes in acoustic impedance between 2 abutting structures. It is generally known that most nerves, including the median nerve, are surrounded by hyperechoic structures such as the tendons and that these hyperechoic structures may affect their appearance. Further investigation is required to clarify these findings in larger groups of diabetic patients using other modalities, such as magnetic resonance imaging.

Finally, there is little doubt that NCS are widely accepted as more sensitive than US in the evaluation of peripheral nerve disorders. However, US is able to directly show morphological changes in the peripheral nerves. Compared with NUS, US caused less discomfort to patients and was less time-consuming in our study. For these reasons, we promote the possibility of using this technique for the diagnosis of DPN.

8. Acknowledgements

The support of the clinical laboratory staff at the Gifu University Hospital is gratefully acknowledged. Authors also gratefully thank Dr. D. Fukuoka for helpful analysis of the echogenisity in the nerve.

9. References

Abe, M. (2004). Ultrasound measurement of the median nerve for carpal tunnel syndrome of the non-handicapped and the handicapped. J Phys Ther Sci, Vol. 16, No. 2, pp. 107-114, ISSN: 0915-5287.

Albers, JW.; Brown, MB.; Sima, AA.; Greene, DA. (1996). Nerve conduction measures in mild diabetic neuropathy in the Early Diabetes Intervention Trial: the effects of age, sex, type of diabetes, disease duration, and anthropometric factors. Tolrestat Study Group for the Early Diabetes Intervention Trial. Neurology, Vol. 46, No. 1, pp. 85-91, ISSN: 0028-3878.

Alemán, L.; Berná, JD.; Reus, M.; Martínez, F.; Doménech-Ratto, G.; Campos, M. (2008). Reproducibility of sonographic measurements of the median nerve. J Ultrasound Med, Vol. 27, No. 2, pp. 193-197, ISSN: 0278-4297.

Attarian, S.; Azulay, JP.; Boicraut, J.; Escande, N.; Pouget, J. (2001). Terminal latency index and modified F ratio in distinction of chronic demyelinating neuropathies. Clin Neurophysiol, Vol. 112, No. 3, pp. 457-463, ISSN: 1388-2457.

Cameron, NE.; Eaton, SE.; Cotter, MA.; Tesfaye, S. (2001). Vascular factors and metabolic interactions in the pathogenesis of diabetic neuropathy. Diabetologia, Vol. 44, No. 11, pp. 1973-1988, ISSN: 0012-186X.

Cartwright, MS.; Chloros, GD.; Walker, FO.; Wiesler, ER.; Cambell, WW. (2007). Diagnostic ultrasound for nerve transection. Muscle Nerve, Vol. 35, No. 6, pp. 796-799, ISSN: 0148-639X.

Chudzik, W.; Kaczorowska, B.; Przybyła, M.; Chudzik, B.; Gałka, M. (2007). Diabetic neuropathy. Pol Merkur Lekarski, Vol. 22, No. 127, pp. 66-69, ISSN: 1426-9686.

Colak, A.; Kutlay, M.; Pekkafali, Z.; Saraçoglu, M.; Demircan, N.; Simşek, H.; Akin, ON.; Kibici, K. (2007). Use of sonography in carpal tunnel syndrome surgery: a prospective study. Neurol Med Chir, Vol. 47, No. 3, pp. 109-115, ISSN: 1349-8029.

Cornblath, DR.; Chaudhry, V.; Carter, K.; Lee, D.; Seysedadr, M.; Miernicki, M.; Joh, T. (1999). Total neuropathy score: validation and reliability study. Neurology, Vol. 53, No. 8, pp. 1660-1664, ISSN: 0028-3878.

Diabetes Control and Complications Trial (DCCT) Research Group. (1995). Effect of intensive diabetes treatment on nerve conduction in the Diabetes Control and Complications Trial. Ann Neurol, Vol. 38, No. 6, pp. 869-880, ISSN: 034-5134.

Duncan, I.; Sullivan, P.; Lomas, F. (1999). Sonography in the diagnosis of carpal tunnel syndrome. AJR Am J Roentgenol, Vol. 173, No. 3, pp. 681-684, ISSN: 0361-803X.

Dyck, PJ.; Karnes, JL.; Daube, J.; O'Brien, P.; Service, FJ. (1985). Clinical and neuropathological criteria for the diagnosis and staging of diabetic polyneuropathy. Brain, Vol. 108, No. 4, pp. 861-880, ISSN: 0006-8950.

Dyck, PJ. (1988). Detection, characterization, and staging of polyneuropathy: assessed in diabetics. Muscle Nerve, Vol. 11, No. 1, pp. 21-32, ISSN: 0148-639X.

Dyck, PJ.; Kratz, KM.; Lehman, KA.; Karnes, JL.; Melton, LJ 3rd.; O'Brien, PC.; Litchy, WJ.; Windebank, AJ.; Smith, BE.; Low, PA, et al. (1991). The Rochester Diabetic Neuropathy Study: design, criteria for types of neuropathy, selection bias, and reproducibility of neuropathic tests. Neurology, Vol. 41, No. 6, pp. 799-807, ISSN: 0028-3878.

Feldman, EL.; Stevens, MJ.; Thomas, PK.; Brown, MB.; Canal, N.; Greene, DA. (1994). A practical two-step quanttative clinical and electrophysiological assessment for the diagnosis and staging of diabetic neuropathy. Diabetes Care, Vol. 17, No. 11, pp. 1281-1289, ISSN: 0149-5992.

Fornage, BD. (1993). Sonography of peripheral nerves of the extremities. Radiol Med, Vol. 85, No. 5, pp. 162-167, ISSN: 0033-8362.

Greene, DA.; Lattimer, SA.; Sima, AAF. (1987). Sorbitol, phosphoinositides, and sodium-potassium–ATPase in the pathogenesis of diabetic complications. N Engl J Med, Vol. 316, No. 10, pp. 599-606. ISSN: 0028-4793.

Jayaraman, S.; Naidich, TP. (2004). The carpal tunnel: ultrasound display of normal imaging anatomy and pathology. Neuroimaging Clin N Am, Vol. 14, No. 1, pp. 103-113, ISSN: 1052-5149.

Kaplan, P.; Sahgal, V. (1978). Residual latency: new applications of an old technique. Arch Phys Med Rehabil, Vol. 59, No. 1, pp. 24-27, ISSN: 0003-9993.

Karsidag, S.; Morali, S.; Sargin, M.; Salman, S.; Karsidag, K.; Us, O. (2005). The electrophysiological findings of subclinical neuropathy in patients with recently diagnosed type 1 diabetes mellitus. Diabetes Res Clin Pract, Vol. 67, No. 3, pp. 211-219, ISSN: 0168-8227.

Khoury, V.; Cardinal, E.; Bureau, NJ. (2007). Musculoskeletal sonography: a dynamic tool for usual and unusual disorders. AJR Am J Roentgenol, Vol. 188, No. 1, pp. 63-73, ISSN: 0361-803X.

Lee, CH.; Choi, JW.; Kim, KA.; Seo, TS.; Lee, JM.; Park, CM. (2006). Usefulness of standard deviation on the histogram of ultrasound as a quantitative value for hepatic parenchymal echo texture; preliminary study. Ultrasound Med Biol, Vol. 32, No. 12, pp. 1817-1826, ISSN: 0301-5629.

Lee, D.; van Holsbeeck, MT.; Janevski, PK.; Ganos, DL.; Ditmars, DM.; Darian, VB. (1999). Diagnosis of carpal tunnel syndrome, Ultrasound versus electromyography. Radiol Clin North Am, Vol. 37, No. 4, pp. 859-872, ISSN: 0033-8389.

Oates, PJ. (2002). Polyol pathway and diabetic peripheral neuropaathy. Int Rev Neurobiol, Vol. 50, pp. 325-392, ISSN: 0074-7742.

Ogawa, K.; Sasaki, H.; Yamasaki, H.; Okamoto, K.; Matsuno, S.; Shono, T.; Doi, T.; Arimoto, K.; Furuta, H.; Nishi, M.; Nakao, T.; Nanjo, K. (2006). Peripheral nerve functions may deteriorate parallel to the progression of microangiopathy in diabetic patients. Nutr Metab Cardiovasc Dis, Vol. 16, No. 5, pp. 313-321, ISSN: 0939-4753.

Okamoto, M.; Abe, M.; Shirai, H.; Ueda, N. (2000). Diagnostic ultrasonography of the ulnar nerve in cubitial tunnel syndrome. J Hand Surg Br, Vol. 25, No. 5, pp. 499-502, ISSN: 0266-7681.

Osawa, H.; Mori, Y. (1996). Sonographic diagnosis of fatty liver using a histogram technique that compares liver and renal cortical echo amplitudes. J Clin Ultrasound, Vol. 24, No. 1, pp. 25-29, ISSN: 0091-2751.

Otsu, N. (1979). A threshold selection method from gray-level histogram. IEEE Trans. Systems Man Cybern, Vol. 9, No. 1, pp. 62-66, ISSN: 1083-4419.

Peer, S.; Bodner, G.; Meirer, R.; Willeit, J.; Piza-Katzer, H. (2001). Examination of postoperative peripheral nerve lesions with high-resolution sonography. Am J Roentgenol, Vol. 177, No. 2, pp. 415-419, ISSN: 0002-9580.

Perkins, BA.; Bril, V. (2003). Diabetic neuropathy: a review emphasizing diagnostic methods. Clin Neurophysiol, Vol. 114, No. 7, pp. 1167-1175. ISSN: 1388-2457.

Perkins, BA.; Olaleye, D.; Zinman, B.; Bril, V. (2001). Simple screening tests for peripheral neuropathy in the diabetes clinic. Diabetes Care, Vol. 24. No. 2, pp. 250-256, ISSN: 0149-5992.

Radziwill, AJ.; Steck, AJ.; Renaud, S.; Fuhr, P. (2003). Distal motor latency and residual latency as sensitive markers of anti-MAG polyneuropathy. J Neurol, Vol. 250, No. 8 , pp. 962-966, ISSN: 1121-8428.

Redmond, JM.; McKenna, MJ.; Feingold, M.; Ahmad, BK. (1992). Sensory testing versus nerve conduction velocity in diabetic polyneuropathy. Muscle Nerve, Vol. 15, No. 12, pp. 1334-1339, ISSN: 0148-639X.

Said, G. (2007). Diabetic neuropathy: a review. Nat Clin Pract Neurol, Vol. 3, No. 6, pp. 331-340, ISSN: 1745-8358.

Sernik, RA.; Abicalaf, CA.; Pimentel, BF.; Braga-Baiak, A.; Braga, L.; Cerri, GG. (2008). Ultrasound features of carpal tunnel syndrome: a prospective case-control study. Skeletal Radiol, Vol. 37, No. 1, pp. 49-53, ISSN: 0278-4297.

Silvestri, E.; Martinoli, C.; Derchi, LE.; Bertolotto, M.; Chiaramondia, M.; Rosenberg, I. (1995). Echotexture of peripheral nerves: correlation between US and histologic findings and criteria to differentiate tendons. Radiology, Vol. 197, No. 1, pp. 291-296, ISSN: 0033-8419.

Solbiati, L.; De Pra, L.; Ierace, T.; Bellotti, E.; Derchi, LE. (1985). High-resolution sonography of the recurrent laryngeal nerve: anatomic and pathologic considerations. AJR Am J Roentgenol, Vol. 145, No. 5, pp. 989-993, ISSN: 0361-803X.

Stokvis, A.; Van Neck, JW.; Van, Dijke, CF.; Van Wamel, A.; Coert, JH. (2009). High-resolution ultrasonography of the cutaneous nerve branches in the hand and wrist. J Hand Surg Eur, Vol. 34, No. 6, pp. 766-771, ISSN: 2043-6289.

Suzuki, E.; Yasuda, K.; Yasuda, K.; Miyazaki, S.; Takeda, N.; Inouye, H.; Omawari, N.; Miura, K. (1994). 1H-NMR analysis of nerve edema in the streptozotocin-induced diabetic rat. J Lab Clin Med, Vol. 124, No. 5, pp. 627-637, ISSN: 0022-2143.

Thomas, PK. (1997). Classfication, differentiatial diagnosis, and staging of diabetic peripheral neuropathy. Diabetes, Vol.46, No.2, pp. 54-57, ISSN: 0149-5992.

Vincent, AM.; Brownlee, M.; Russell, JW. (2002). Oxidative stress and programmed cell death in diabetic neuropathy. Ann N Y Acad Sci, Vol. 959, pp. 368-383. ISSN: 0077-8923.

Vinik, AI. (1999). Diabetic neuropathy: pathogenesis and therapy. Am J Med, Vol. 107, No. 2, pp. 17S-26S. ISSN: 0002-9343.

Watanabe, T.; Ito, H.; Morita, A.; Uno, Y.; Nishimura, T.; Kato, Y.; Takeda, J.; Seishima, M.; Matsuoka, T. (2009). Sonographic evaluation of the median nerve in diabetic patients: comparison with nerve conduction studies. J Ultrasound Med, Vol. 28, No. 6, pp. 727-734, ISSN: 0278-4297.

Watanabe, T.; Ito, H.; Sekine, A.; Katano, Y.; Nishimura, T.; Kawase, H.; Kato, Y.; Matsuoka, T.; Takeda, J.; Seishima, M. (2010). Sonographic evaluation of the peripheral nerve in diabetic patients: the relationship between nerve conduction studies, echo intensity, and cross-sectional area. J Ultrasound Med, Vol. 29, No. 5, pp 697-708, ISSN: 0278-4297.

Wiesler, ER.; Chloros, GD.; Cartwright, MS.; Smith, BP.; Rushing, J.;Walker, FO. (2006a). The use of diagnostic ultrasound in carpal tunnel syndrome. J Hand Surg Am, Vol. 31, No. 5, pp. 726-732, ISSN: 0363-5023.

Wiesler, ER.; Chloros, GD.; Cartwright, MS.; Shin, HW.; Walker, FO. (2006b). Ultrasound in the diagnosis of ulnar neuropathy at the cubital tunnel. J Hand Surg Am, Vol. 31, No. 5, pp. 1088-1093, ISSN: 0363-5023.

Wild, S.; Roglic, G.; Green, A.; Sicree, R.; King, H. (2004). Global prevalence of diabetes: estimates for the year 2000 and projections for 2030. Diabetes Care, Vol. 27, No. 5, pp. 1047-1053, ISSN: 1047-1053.

Yagihashi, S.; Yamagishi, S.; Wada, R. (2007). Pathology and pathogenetic mechanism of diabetic neuropathy: correlation with clinical signs and symptoms. Diabetes Res Clin Pract, Vol. 77, No. 1, pp. 184-189, ISSN: 1872-8227.

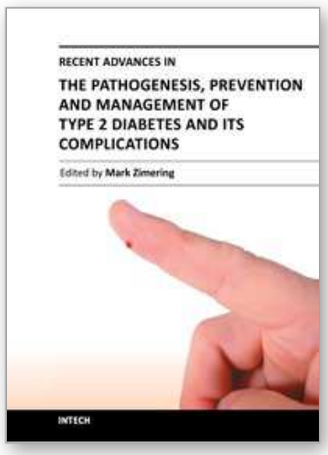

Recent Advances in the Pathogenesis, Prevention and Management of Type 2 Diabetes and its Complications
Edited by Prof. Mark Zimering

ISBN 978-953-307-597-6
Hard cover, 442 pages
Publisher InTech
Published online 29, August, 2011
Published in print edition August, 2011

Type 2 diabetes â€œmellitusâ€ affects nearly 120 million persons worldwide- and according to the World Health Organization this number is expected to double by the year 2030. Owing to a rapidly increasing disease prevalence, the medical, social and economic burdens associated with the microvascular and macrovascular complications of type 2 diabetes are likely to increase dramatically in the coming decades. In this volume, leading contributors to the field review the pathogenesis, treatment and management of type 2 diabetes and its complications. They provide invaluable insight and share their discoveries about potentially important new techniques for the diagnosis, treatment and prevention of diabetic complications.

How to reference
In order to correctly reference this scholarly work, feel free to copy and paste the following:

Tsuneo Watanabe, Shin-ichi Kawachi and Toshio Matsuoka (2011). Sonographic Imaging of the Peripheral Nerves in Patients with Type 2 Diabetes Mellitus, Recent Advances in the Pathogenesis, Prevention and Management of Type 2 Diabetes and its Complications, Prof. Mark Zimering (Ed.), ISBN: 978-953-307-597-6, InTech, Available from: http://www.intechopen.com/books/recent-advances-in-the-pathogenesis-prevention-and-management-of-type-2-diabetes-and-its-complications/sonographic-imaging-of-the-peripheral-nerves-in-patients-with-type-2-diabetes-mellitus

INTECH
open science | open minds

InTech Europe
University Campus STeP Ri
Slavka Krautzeka 83/A
51000 Rijeka, Croatia
Phone: +385 (51) 770 447
Fax: +385 (51) 686 166
www.intechopen.com

InTech China
Unit 405, Office Block, Hotel Equatorial Shanghai
No.65, Yan An Road (West), Shanghai, 200040, China
中国上海市延安西路65号上海国际贵都大饭店办公楼405单元
Phone: +86-21-62489820
Fax: +86-21-62489821

IntechOpen